LWT - Food Science and Technology 96 (2018) 551–559

Contents lists available at ScienceDirect

LWT - Food Science and Technology

journal homepage: www.elsevier.com/locate/lwt

Developing model food systems with rice based products for microwave assisted thermal sterilization

Thammanoon Auksornsri[a], Ellen R. Bornhorst[b,**], Juming Tang[b,*], Zhongwei Tang[b], Sirichai Songsermpong[a]

[a] Department of Food Science and Technology, Faculty of Agro-Industry, Kasetsart University, Bangkok, 10900, Thailand
[b] Department of Biological Systems Engineering, Washington State University, Pullman, WA, 99164-6120, USA

ARTICLE INFO

Keywords:
Rice
Maillard browning
Imaging
Thermal processing
Commercial sterilization

ABSTRACT

Model foods are effective tools to evaluate heating patterns and determine hot and cold spot locations in food packages during microwave-assisted thermally sterilization (MATS) processes. Previous research on model food development has focused on high-moisture foods, with limited information on medium-moisture foods (0.2–0.6 g water/g food). This research aimed to develop rice model foods to simulate medium-moisture food during MATS processing. The optimal composition of a rice flour gel (RFG) model food was 0.3 g/g rice flour, 0.135 g/g tapioca starch, 0.001 g/g xanthan gum, 0.005 g/g D-ribose, and 0.559 g/g water, and a rice to water ratio of 1:1.2 g/g with 0.005 g/g D-ribose for the rice grain (RG) model. The temperature sensitivities of the models' color parameters could be applicable for safety and quality attribute modeling; the RFG model had a larger range of z-values (11–31 °C) than the RG model (18–27 °C). Validation results showed that the RG model food received more thermal energy than the RFG model, with thermal treatment equivalents at 121 °C of 60.3 and 6.5 min, respectively. The heating pattern in RFG medium-moisture model food was consistent with high-moisture models in MATS processing. Model foods developed in this research could be helpful tools for microwave process development for medium-moisture foods.

1. Introduction

Rice is an important staple food in Thailand and many other Asian countries (Srichamnong, Thiyajai, & Charoenkiatkul, 2016). In 2016, the world production of milled rice increased considerably by 498 million tonnes and consumption also increased by 501 million tonnes (World Food Situation, 2016). Jasmine rice (*Oryza sativa* L.) is one of the most popular varieties of rice in Thailand due to its excellent quality; it has a unique aromatic fragrance, white color like the jasmine flower, soft and tender texture, and good taste. Jasmine rice is the primary rice cultivar for domestic consumption in Thailand and a major export commodity, which is important for Thailand's economic growth (Leelayuthsoontorn & Thipayarat, 2006; Phanchaisri et al., 2007). With the increasing popularity of ready-to-eat (RTE) meals, Jasmine rice is often selected as a side-dish in shelf-stable, chilled, and frozen RTE products. Shelf-stable RTE rice is currently produced by conventional thermal processing (Byun et al., 2010). However, the severe thermal treatment of conventional processes needed to achieve commercial sterility may cause degradation of quality attributes; this yields shelf-stable RTE rice products that are dry or clumped together with a burnt flavor, yellowed color, and degraded heat-labile nutrients (Narkrugsa & Saeleaw, 2009).

Microwave heating has been studied to replace conventional heating methods for various food processing applications. The rapid, volumetric heating of microwave energy can help overcome one of the main drawbacks of conventional thermal processes: long thermal processing time due to slow heat transfer rates (Tang, 2015). Microwave-assisted thermal sterilization (MATS) technology has been developed at Washington State University (WSU) to commercially sterilize pre-packaged foods. The MATS technology was accepted by the U.S. Food and Drug Administration (FDA) for commercial sterilization of mashed potatoes and salmon fillets in Alfredo sauce and received a non-objection notice from the U.S. Department of Agriculture Food Safety and Inspection Service (USDA-FSIS) for commercial sterilization of pre-packed foods containing meat, poultry, and eggs (Tang, 2015). The heating time in MATS is substantially shorter than that of a conventional retort process; this reduction in heating time using MATS yields commercially sterile food products with superior quality (Pandit, Tang,

* Corresponding author.
** Corresponding author.
E-mail addresses: ellen.bornhorst@wsu.edu (E.R. Bornhorst), jtang@wsu.edu (J. Tang).

https://doi.org/10.1016/j.lwt.2018.05.054
Received 16 June 2017; Received in revised form 22 May 2018; Accepted 24 May 2018
Available online 24 May 2018
0023-6438/

Mikhaylenko, & Liu, 2006; Zhang, Tang, Liu, Bohnet, & Tang, 2014). The standard procedure for developing in-package MATS processes requires an appropriate model food with chemical marker precursors to determine cold spots in food packages. Mobile temperature sensors are then used to determine temperature profiles at the cold spots in real foods that have similar heating patterns in a MATS system. The temperature histories are used in lethality calculations to select process parameters (Tang, 2015).

A chemical marker method was developed at the U.S. Army Natick Soldier Research Center that provides a rapid, accurate, and reliable method to determine the heating pattern and locate the hot and cold spots in foods processed with thermal sterilization (Kim & Taub, 1993). This method is based on the development of brown color through the Maillard browning reaction between amino acids and reducing sugars. Three chemical markers (M-1, M-2, and M-3) are formed during the Maillard reaction and were identified as potential time-temperature indicators with strong correlations to thermal lethality (Pandit, Tang, Liu, & Pitts, 2007a; Pandit et al., 2006; Tang, 2015; Zhang et al., 2014). M-2 (4-hydroxy-5-methyl-3(2H)-furanone) was found to be more appropriate for high temperature and short time processing (e.g. microwave sterilization) due to faster formation and first order kinetics, whereas M-1 (2,3-dihydro-3,5-dihydroxy-6-methyl-4(H)-pyran-4-one) was suitable for longer processes, such as pasteurization, radio frequency sterilization, ohmic heating, and canning (Pandit et al., 2006; Tang, Feng, & Lau, 2002; Wang, Lau, Tang, & Mao, 2004).

Using the chemical marker technique in real foods is problematic, as real foods are mostly non-homogenous, which can lead to inaccurate heating pattern detection (Wang et al., 2004). Therefore, various model foods were developed to simulate real foods in order to accurately predict the location of cold and hot spots in microwave processed foods (Zhang et al., 2015). Previous work on model foods for microwave processing applications include the development of whey protein gel (Lau et al., 2003), mashed potato with xanthan gum (Pandit et al., 2006), low-acyl gellan gel (Zhang et al., 2015), mashed potato with gellan gum (Bornhorst, Tang, Sablani, & Barbosa-Cánovas, 2017b), egg white gel (Zhang, Liu, Nindo, & Tang, 2013), and agar gel (Sakai, Mao, Koshima, & Watanabe, 2005). Model foods have been used to emulate real foods, such as mashed potato, macaroni and cheese (Wang, Wig, Tang, & Hallberg, 2003), salmon fillet (Wang et al., 2009), sliced beef in gravy (Tang et al., 2008) and sea cucumber (Cong, Liu, Tang, & Xue, 2012).

Quantifying M-1 and M-2 in model foods requires expensive and time-consuming analyses with high performance liquid chromatography (HPLC) (Pandit, Tang, Liu, & Mikhaylenko, 2007b; Zhang et al., 2014). According to Pandit et al. (2007b), two people spent 2.5 days to analyze M-2 concentrations at 40 unique locations to create a 3-D heating pattern of the M-2 distribution in one tray of mashed potato model food that was processed with MATS. Creating heating patterns with this labor-intensive HPLC analysis is not practical, especially when conducting MATS process development that requires many tests, replicated with multiple trays (Pandit et al., 2007b). For this reason, more rapid methods using computer vision systems with image analysis were developed to quantify brown color formation (Bornhorst et al., 2017b; Pandit et al., 2007b). Brown color formation in the model food systems has also been shown to be a direct result of the Maillard reaction (Bornhorst et al., 2017b) and color quantification through image analysis has been shown to produce heating pattern results comparable to that generated by quantification of chemical marker M-2 (Pandit et al., 2007a, 2007b).

All previously mentioned research on model food development and simulation of real foods has been for high moisture foods. There are no existing model foods that could be used to simulate medium moisture food products, such as rice or pasta. There is a need to develop new model food systems to simulate medium moisture foods for heating pattern determination of MATS processed food. The objectives of this research were to (1) determine the optimal composition for rice model food systems, (2) determine the color change kinetics of the ideal model food systems, and (3) conduct a validation with MATS.

2. Materials and methods

2.1. Model food formula development

Two types of rice based model food systems were developed in this study: whole rice grains (RG) and rice flour gel (RFG). In developing the rice grain (RG) model food system, three rice to water ratios were tested in a preliminary study to determine which would have the optimal texture that was not too sticky and not too hard. One hundred grams of Jasmine rice grains with rice to water ratios of 1:1 g/g, 1:1.2 g/g, and 1:1.5 g/g were cooked in a water bath for 40 min at 95 °C. These rice to water ratios and cooking time were selected based on typical procedures used for cooking jasmine rice (Crowhurst & Creed, 2001). The consistency and texture of the samples were evaluated. The results were used to plan further development of RG systems.

Preliminary studies were also conducted to select the appropriate formulation to create the RFG model food. The rice flour used in this study was made from dry milled Thai Jasmine rice (*Oryza sativa*, CP. Intertrade, Pathumthani, Thailand) using a Vitamix blender (G-series, Vitamix Corporation, Cleveland, Ohio, USA), followed by sieving through a 0.15 mm standard sieve (Advantech, New Berlin, WI, USA). Different concentrations of rice flour, 15, 20, 25 and 30 g/100 g, were selected to make the RFG model foods. The suspension (mixture of rice flour and distilled water) was mixed continuously for 3 h at room temperature (22 °C) using magnetic stirring to achieve homogeneity. The mixture was then heated at 95 °C in a water bath for 40 min to set the gel. Preliminary tests showed that the mixtures with 25–30 g/100 g rice flour could form gels, but the gels were not strong enough and were difficult to cut. Tapioca starch (Walong Marketing Inc, Buena Park, CA, USA) and xanthan gum (Sigma-Aldrich, St. Louis, MO, USA) were added into the 25–30 g/100 g RFG formulations (Table 1) in order to improve the texture of the gels and to create more rigid, stable gels.

Tapioca starch, produced from cassava roots, was selected as an ingredient for the RFG system because it is widely used as a food ingredient for textural and shape modifications; it can function as a thickener, stabilizer, gelling and bulking agent, and water retention agent (Nawab, Alam, Haq, & Hasnain, 2016). Tapioca starch has high viscosity, clear appearance, and low production cost, compared to other starches, especially in Southeast Asia. However, the viscosity of a tapioca starch paste decreases when mechanically disturbed, which leads to a low textural stability during storage (Pongsawatmanit & Srijunthongsiri, 2008). The addition of hydrocolloids can improve or maintain desirable textural properties and stability of tapioca starch due to the modification of the starch gelatinization and retrogradation behaviors (Sae-kang & Suphantharika, 2006). Xanthan gum has been widely used in combination with starch in foods because it improves the physical properties of various starch pastes and gels. The addition of xanthan gum can help increase viscosity, increase water holding capacity, improve film formation and freeze-thaw stability, and decrease retrogradation, syneresis, and ice crystallization (Nawab et al., 2016; Sae-kang & Suphantharika, 2006). Xanthan gum also has excellent stability under heat and acidic conditions (Nawab et al., 2016;

Table 1
Nine formulations (g/100 g) of the rice flour gel model foods.

Ingredients	1	2	3	4	5	6	7	8	9
Water	66.2	66.1	64.1	59.2	59.1	55.6	54.2	54.1	54.1
Rice flour	25.0	25.0	25.0	30.0	30.0	30.0	30.0	30.0	35.0
Tapioca starch	8.0	8.0	10.0	10.0	10.0	13.5	15.0	15.0	10.0
D-ribose	0.5	0.5	0.5	0.5	0.5	0.5	0.5	0.5	0.5
Salt	0.3	0.3	0.3	0.3	0.3	0.3	0.3	0.3	0.3
Xanthan gum	–	0.1	0.1	–	0.1	0.1	–	0.1	0.1

Pongsawatmanit & Srijunthongsiri, 2008).

In order to facilitate brown color formation from the Maillard reaction, D-ribose (Sigma-Aldrich, St. Louis, MO, USA) was added to the distilled water that was used to prepare both RG and RFG model foods. Preliminary tests were conducted to determine the ideal concentration of D-ribose for color analysis during heating pattern visualization of MATS processed model foods. The tests examined 0.2, 0.5, 1.0 and 1.5 g/100 g D-ribose additions in the samples. After the model foods were prepared, both RFG and RG were filled and sealed in thermal kinetic testing (TKT) cells designed at Washington State University (Zhang et al., 2014). The TKT cells were heated in an oil bath with ethylene glycol as the heating medium (Haake DC 30, Thermo Fisher Scientific Inc., Newington, NH, USA). Preliminary studies to determine the ideal formula were conducted at 121 °C for 5, 10, 20 or 40 min, followed by cooling the samples in ice water (0 °C). A calibrated type-T thermocouple (Omega Engineering, Norwalk, CT, USA) was used to measure the sample temperature during heating and determine the come-up time, which was defined as the time when the sample cold spot (geometric center) was within 0.5 °C of the target temperature (Bornhorst et al., 2017b). The come-up time was measured as 4.3 min for RFG and 4.5 min for RG model food systems.

2.2. Color change kinetic study

Based on the results of the preliminary tests, RFG formula 6 (see Table 1) with 0.5 g/100 g D-ribose and RG with a rice to water ratio of 1:1.2 g/g with 0.5 g/100 g D-ribose were selected as the optimal model foods to be utilized in the color change kinetic study. Rice model foods were filled and sealed in custom built, disk-shaped, aluminum test cells with a diameter of 18 mm and height of 4 mm (Chung, Birla, & Tang, 2008). The test cells were heated at 116, 121 and 126 °C with an oil bath using ethylene glycol as the heating medium (Haake DC 30, Thermo Fisher Scientific Inc., Newington, NH, USA) followed by cooling in ice water (0 °C). The tested temperatures covered the range of process temperatures used in MATS processes. Heating times included 5, 10, 15, 30, 45, 60 and 75 min, excluding the come-up time of 2.7, 3.1, and 3.4 min for RFG and 2.9, 3.3, and 3.5 min for RG model food systems at 116, 121 and 126 °C, respectively. The above time span covered processing times used in MATS and conventional canning processes. A calibrated type-T thermocouple (Omega Engineering, Inc., Norwalk, CT, USA) was used to measure the sample temperature during heating. Kinetic experiments were conducted in triplicate.

The color was determined in L*a*b* (CIELAB) color space using a computer vision system with hard-ware according to Pandit et al. (2007b). Briefly, a Nikon D 70 (Nikon Instrument, Melville, NY, USA) digital camera with 18–70 mm DX Nikon lens was fit on top of a light pod. Nikon Capture 4 Editor version 4.3.0 software (Nikon Instrument, Melville, NY, USA) was used to acquire and download the images to a Dell Workstation. The camera settings and image analysis were based on Bornhorst et al. (2017b). Briefly, image analysis was performed in MATLAB R2013a, including a color correction using a color reference card (QPcard 203, QPcard AB, Helsingborg, Sweden) and color analysis of a circle containing the majority of the sample (37,695 pixel values).

Color was expressed using several different parameters: L*, a*, and b* values, grayscale, and total color change. Total color change (ΔE) was determined by Hunter (1975):

$$\Delta E = \sqrt{(L_t^* - L_0^*)^2 + (a_t^* - a_0^*)^2 + (b_t^* - b_0^*)^2} \quad (1)$$

where L_t^* is the L* value at time t, L_0^* is the L* value at time 0 (initially), a_t^* is the a* value at time t, a_0^* is the a* value at time 0, b_t^* is the b* value at time t, and b_0^* is the b* value at time 0.

Statistical analyses of the data were performed using SAS® 9.2. Correlations between the color values (L*, a*, b*, grayscale and ΔE) and heating time were determined by Pearson correlation coefficients. The p-value for significance was less than 0.05. The reaction order, reaction constants (k) and activation energy (E_a) of color values were determined by a two-step modified non-linear regression method described in Lau et al. (2003) and Bornhorst et al. (2017b). Briefly, step one fit zero, first, and second order rate equations to the data using non-linear regression. For example, the generalized first order equation was (Lau et al., 2003):

$$C = C_\infty - (C_\infty - C_0) \exp(-kt) \quad (2)$$

where C is the value of the color parameter (L*, a*, b*, grayscale or ΔE), C_∞ is the value of the parameter at saturation, C_0 is the initial value of the parameter, k is the reaction rate constant (1/min), and t is time (min). Step two utilized a standard linear regression to describe the effect of temperature change on the reaction rate constants using the Arrhenius equation. Coefficients of determination (R^2) were calculated for each regression. The best fit order of reaction (zero, first, or second order) in step one was ascertained based on the highest coefficients of determination.

2.3. Validation with MATS

A validation was conducted to assess the effectiveness of rice model food systems in determining the heating pattern and locations of the cold and hot spots experienced in a MATS process. Sample trays contained 300 g of RFG model food or whole RG model food in plastic trays (14 cm × 9.5 cm x 3 cm). Validation experiments were conducted in triplicate using a 915 MHZ single-mode MATS system developed at WSU (Tang, Liu, Patfiak, & Eves, 2006). This system consisted of four processing sections: pre-heating, microwave heating, holding, and cooling. The trays of model food were first pre-heated in 61 °C water for 30 min in the preheating section. The trays were then moved through the microwave heating cavities and were heated by both microwave energy and hot water (122 °C) for 5.1 min. The trays were moved through the holding section (5.2 min residence time for each tray) in hot water (122 °C). Finally, the trays were moved to the cooling section, cooled down for 5 min in 20 °C water, and removed from the MATS system. Rapid cooling was necessary in order to stop further progression of the Maillard reaction and harden the model food gel to make it easier to cut into layers.

The processed rice model food samples were cut into horizontal and vertical layers for heating pattern detection. A sharp, stainless-steel slicing knife (25 cm) and custom-designed polypropylene plastic cutting jigs were used to cut the model foods in the middle layers. For consistency, the thickness of all model food samples was controlled by using the same sample weights and packaging conditions. However, the variations in the model food slice thickness after processing was not expected to influence the results because the rice model foods were opaque and not translucent (Bornhorst et al., 2017b).

In order to analyze the heating pattern and visualize the hot and cold spots, digital images of the cut layers were taken using a computer vision system, as described above in section 2.2. Briefly, the system included a light pod, compact fluorescent light bulbs, a Nikon D 70 digital camera (F-11, 1/15 s, ISO 200, white balanced), and a computer with image acquisition software (Bornhorst et al., 2017b; Pandit et al., 2007b). Heating patterns inside the food samples were analyzed and color mapped images were created using a custom-developed script in an NI vision development module program, as described in Pandit et al. (2007b).

After conducting preliminary MATS runs and analyzing the image results, the hot and cold spots in the trays of model foods were determined. As described in Bornhorst, Liu, Tang, Sablani, & Barbosa-Cánovas (2017a), both cold and hot spot temperatures were measured to ensure safety (cold spot) and give an indication of quality (hot spot). Temperatures were measured every 2 s during MATS processing using wireless, calibrated, mobile metallic Ellab temperature sensors and data logging software (Ellab Inc., Centennial, CO, USA) (Luan, Tang,

Pedrow, Liu, & Tang, 2013); these sensors have a reported uncertainty of ± 0.1 °C in the range of −20 to 140 °C. Two separate MATS runs were conducted, during which cold and hot spot temperatures were measured in separate packages for both the RFG and RG model foods (4 sensors in 4 different packages per run).

3. Results and discussion

3.1. Selection of optimal rice model food systems

Nine formulas of RFG model foods were developed and tested (Table 1). Preliminary results showed that formulas 1, 2, and 3 with the lowest amounts of added rice flour and starch formed weaker, sticky gels that were difficult to cut into layers. Conversely, formulas 7, 8, and 9 with the highest amounts of added rice flour and starch resulted in a texture that was brittle, too hard, and difficult to slice into layers. A medium level of added rice flour and starch in formulas 4, 5, and 6 resulted in the ideal model food texture that was easy to slice into 3 layers. Among formulas 4–6, formula 6 had the largest amount of tapioca starch and added xanthan gum, which yielded a model food with a better gel quality compared to formulas 4 and 5. This result could be explained by the known benefit of adding xanthan gum to tapioca starch suspensions; the addition of xanthan gum causes a synergistic increase in viscosity due to the decreased availability of unbound water (Chantaro & Pongsawatmanit, 2010) and the reduction of syneresis (Sae-kang & Suphantharika, 2006). By utilizing both tapioca starch and xanthan gum, the physical properties of the RFG model food were improved. Additionally, the moisture content of formula 6 was measured to be 59.2 g water/100 g food material (wet basis), which was similar to that of cooked rice (58.2 g water/100 g food material (wet basis)). When creating model foods to emulate real foods with medium moisture, having similar model food and real food moisture contents was of critical importance. Therefore, formula 6 was selected as the RFG model food for further study.

Three formulas of whole RG model foods with varying amounts of added water were developed and tested. Preliminary results showed that a rice grains to water ratio of 1:1.2 g/g was the ideal amount of added water in this model food system. This amount of added water yielded rice grains with a uniform shape and appearance that were not too soggy or dry compared to the 1:1 or 1:1.5 g/g ratios. The moisture content of the ideal RG model food was similar to cooked rice, with the RG model food having a moisture content of 58.3 g water/100 g food material (wet basis) compared to cooked rice (58.2 g water/100 g food material (wet basis)).

Concentration of D-ribose, a precursor in the Maillard reaction, was also varied from 0.2 to 1.5 g/100 g in preliminary studies to determine the optimal formulation. Brown color formation in both the RG model food system and RFG model food increased with increasing D-ribose concentration during heating at sterilization temperatures. In both rice model systems, 0.5 g/100 g D-ribose was selected as the ideal formula with adequate brown color formation during heating. The formula with the lowest amount of added D-ribose, 0.2 g/100 g, did not have adequate brown color formation to be quantified using image analysis, especially at the lower temperature of 116 °C. Formulas with higher amounts of added D-ribose, 1.0 and 1.5 g/100 g, are not as advantageous because there was too much color change, especially at the higher temperature of 126 °C. Additionally, chemical-grade D-ribose is the most expensive ingredient in the model food systems and it was preferable to select the lowest level of added D-ribose that produced a quantifiable color change for cost effectiveness. Therefore, the formula with 0.5 g/100 g added D-ribose was chosen as the ideal model food system. Preliminary results showed this model food formulation had quantifiable brown color development during heating that could be applicable for heating pattern visualization for thermal sterilization. The addition of 0.5 g/100 g D-ribose to the model food formulation is within the range of added ribose found in previous work on high moisture model food development for thermal sterilization applications, with 0.5–1 g/100 g added D-ribose in whey protein model food (Cong et al., 2012; Gupta, Mikhaylenko, Balasubramaniam, & Tang, 2011; Lau et al., 2003; Wang et al., 2009) and 1.5 g/100 g added D-ribose in mashed potato model food (Pandit et al., 2006).

Previous work by Auksornsri, Tang, Tang, Lin, and Songsermpong (2018) investigated the dielectric properties (dielectric constants and loss factors) and penetration depths of RFG and RG model foods with different D-ribose (0.2, 0.5 and 1 g/100 g) and salt contents (0, 0.3, 0.5, 1, 1.5, 2 and 3 g/100 g) and of cooked rice (CR) over a frequency range of 300–3000 MHz at temperatures from 20 to 121 °C. Result showed that the dielectric properties of rice models with 0 g/100 g salt and 0.5 g/100 g D-ribose closely matched the properties of CR; this indicated that rice model foods could be used to emulate CR for heating pattern and cold/hot spot detection in the development of microwave sterilization processes at 915 MHz and 2450 MHz.

3.2. Color change during heating

Color change of rice model foods (RFG and RG) after heat treatment at different temperatures was analyzed using a computer vision system. Both rice model foods showed increasing brown color intensity with increasing heating time and temperature until an apparent color saturation was reached (Fig. 1). Image analysis was utilized to quantify the color changes and correlation analysis was utilized to determine which color parameters could be employed as time-temperature indicators. Experimental L*, a*, grayscale and ΔE values for RFG and RG models during heating at each temperature were shown in Fig. 2 and Fig. 3. Statistical analyses of the color images for heat treated RFG and RG model foods showed the correlation strength between heating time and L*, a*, b*, grayscale, and ΔE at each temperature. For all temperatures, strong and significant correlations were found between the heating time and all color parameters ($P < 0.05$), except b* for RFG and RG at 121 and 126 °C. Correlation coefficients for rice model food systems ranged from −0.99 to −0.94 for L*, 0.89 to 0.98 for a*, 0.49 to 0.85 for b*, −0.99 to −0.93 for grayscale, and 0.78 to 0.92 for ΔE. Negative correlations for L* and grayscale indicated that the parameter value decreased with increasing heating time, showing a darker color over time. Positive correlations for a* and total color change indicated that the parameter value increased with increasing heating time, showing a more red color with more total color change after longer times. L*, a*, grayscale, and ΔE were selected for further analysis because these parameters had strong and significant correlations with heating time and temperature, while b* was excluded due to lack of strong correlations for the majority of treatment temperatures. The lack of correlation among b* and heating time matched previous work reported by Bornhorst et al. (2017b) on model foods for pasteurization applications.

Results showed that in both rice model food systems the color formation, expressed as L*, a*, grayscale, and ΔE, fit best to first-order reaction kinetics at all temperatures, with the highest R^2 values for all models and treatments. When the data were fit to zero order kinetics, the average R^2 among all model and treatments was 0.87, with a range of 0.61–0.97 compared to an average of 0.98 and a range of 0.96–0.99 for first order, an average of 0.84 and a range of 0.10–0.97 for second order. A first order fit matched results obtained for the formation of color values (L* and a*) in egg white gel, mashed potato gel and gellan gel (Bornhorst et al., 2017b), the formation of M-2 in whey protein gels (Gupta et al., 2011; Lau et al., 2003) and mashed potato (Pandit et al., 2006), and the formation of M-1 in whey protein gel (Wang et al., 2004).

For each color parameter, L*, a*, grayscale, and ΔE, the reaction rate (k) at each temperature was calculated along with the activation energy (E_a) for the temperature range 116–126 °C (Tables 2 and 3). For ease of using the results in future studies and comparison to previous work, D and z-values were also calculated from k and E_a, respectively.

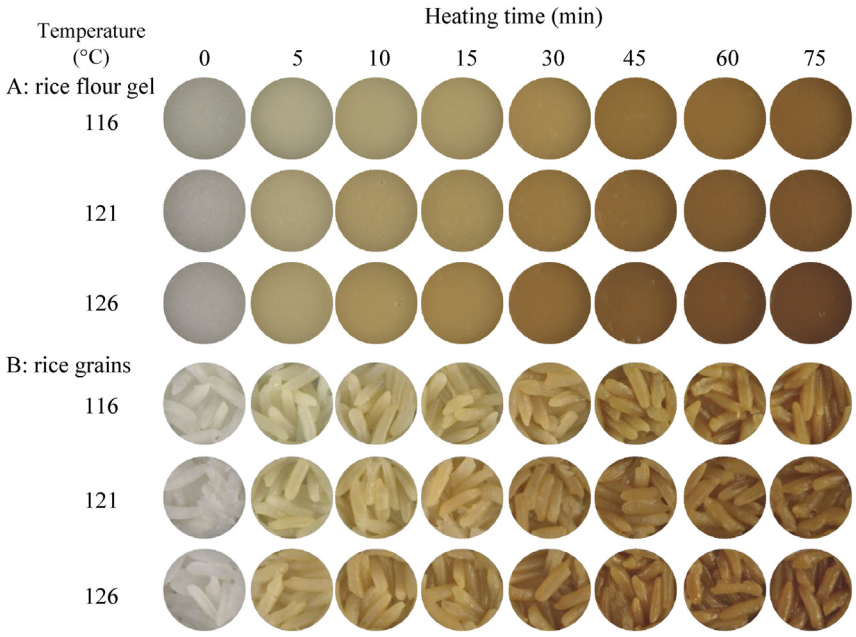

Fig. 1. Color changes in rice flour gel (A) and rice grain (B) model foods (0.5 g/100 g D-ribose, 0 g/100 g salt) after 0–75 min heating at 116, 121, and 126 °C. (For interpretation of the references to color in this figure legend, the reader is referred to the Web version of this article.)

For all temperatures and color parameters, the RG model food had slower color formation and smaller D-values compared to the RFG model food. This result could be explained by differences in formulation; perhaps there was an increased availability of sugars and amino acids for participation in the Maillard reaction in the RFG model food because the rice was ground into flour instead of using whole rice grains (RG model food). Previous work by Bornhorst et al. (2017b) supports the idea that formulation differences, too low of pH, reactant availability, or reactants with insufficient concentrations to catalyze the reaction, all impact the brown color formation. For example, when no ribose or lysine were added, there was no significant brown color or chemical marker formation (Bornhorst et al., 2017b).

As expected, the reaction rates for all color parameters increased with increasing temperature and fit well to an Arrhenius equation with an average R^2 value of 0.98 and a range of 0.95–0.99 among all treatments. This trend matched the results for Maillard reaction kinetics reported by Lau et al. (2003), Wang et al. (2004) and Pandit et al. (2006). The RG model food had larger L* and grayscale z-values than the RFG model food, with L* z-values of 27 ± 2 and 11 ± 2 °C and grayscale z-values of 27 ± 1 and 15 ± 1 °C for RG and RFG, respectively. This result indicates that the color change of the RG model food, in terms of light-dark (L*, grayscale), was less sensitive to temperature change than the RFG model food. The a* z-values for both model foods were similar, 18 ± 4 for RG and 20 ± 3 °C for RFG, indicating a similar temperature sensitivity for the red-green color. The overall color change, ΔE z-value exhibited a different trend, with RG having a smaller z-value (24 ± 2 °C) than RFG (31 ± 2 °C). Color parameters with different temperature sensitivities within a model food could be levered during future image analysis and heating pattern visualization work, as multiple safety and/or quality attributes could be simulated using one model food (Bornhorst, Tang, Sablani, & Barbosa-Cánovas, 2017c, Bornhorst, Tang, Sablani, & Barbosa-Cánovas, 2017d). The concept of using multiple color components (L*, a*, grayscale, and ΔE) for heating pattern visualization was employed in previous work on microwave-assisted pasteurization (Bornhorst et al., b, c, d, 2017a); however, this idea has not been applied to higher temperature

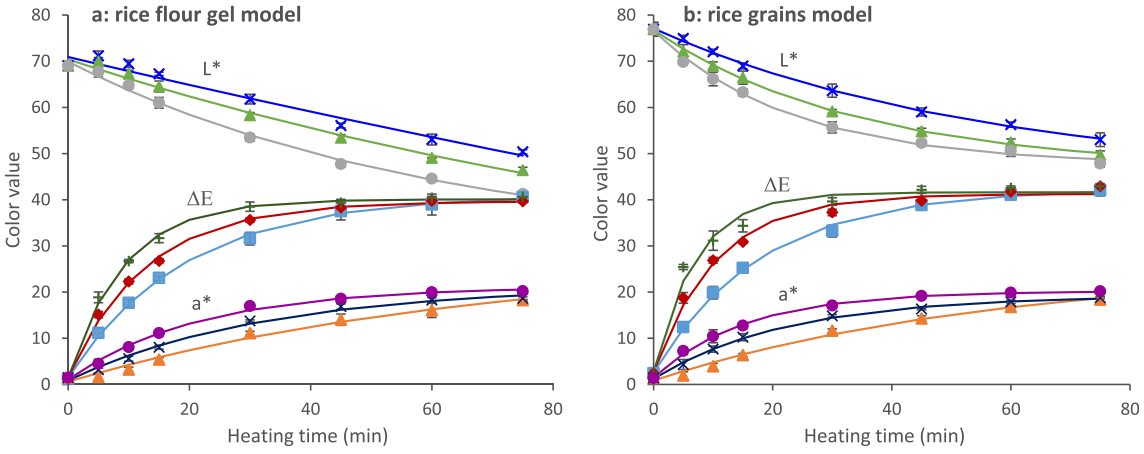

Fig. 2. Experimental L*, a*, and ΔE values (average ± 95% confidence interval) for rice flour gel (a) and rice grains (b) models during heating at 116, 121 and 126 °C. For both model foods, L* values are shown for 116 °C (×), 121 °C (▲), and 126 °C (●); ΔE are shown for 116 °C (■), 121 °C (◆), and 126 °C (+); and a* values are shown for 116 °C (▲), 121 °C (×), and 126 °C (●). Predicted color values using the first order kinetic model are shown (——). (For interpretation of the references to color in this figure legend, the reader is referred to the Web version of this article.)

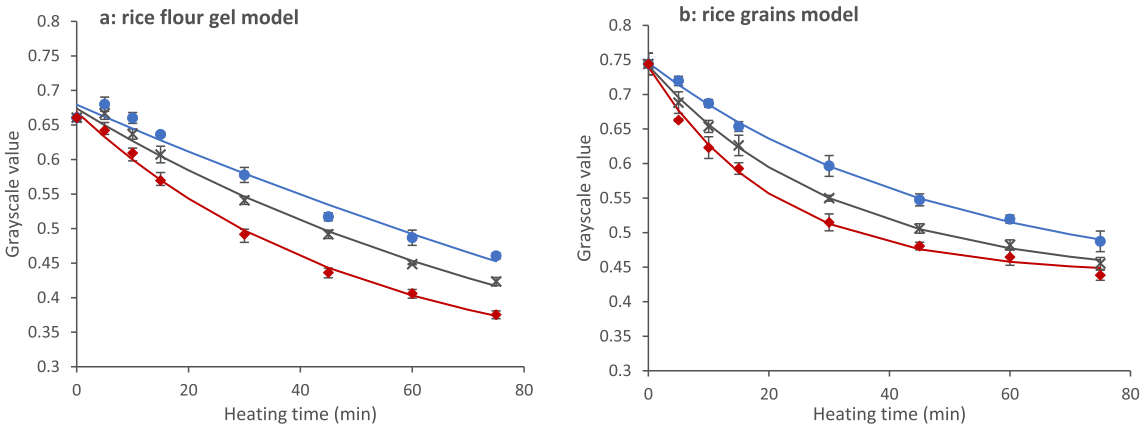

Fig. 3. Experimental grayscale values (average ± 95% confidence interval) for rice flour gel (a) and rice grains (b) models during heating at 116 °C (●), 121 °C (×) and 126 °C (◆). Predicted color values using the first order kinetic model are shown (——). (For interpretation of the references to color in this figure legend, the reader is referred to the Web version of this article.)

processes (microwave-assisted thermal sterilization), which has typically only considered grayscale value during image analysis (Pandit et al., 2007b, 2007a; Zhang et al., 2014).

The RFG model food had a larger range of z-values for all the color parameters (11–31 °C) compared to a range of 18–27 °C for the RG model. Understanding the range of z-values is important to guide the model food selection for future work; a larger range of temperature sensitivities and reactions rates is preferred in order to have more flexibility in matching safety or quality attribute changes with color changes in the model food (Bornhorst et al., 2017b). These z-value ranges could be applicable to simulate the temperature sensitivity of both pathogen and food quality degradation (Holdsworth, 1997, p. 283).

3.3. Validation with MATS

The heating patterns in rice model foods sterilized by a MATS process were analyzed using a computer vision system. Color change was visualized using color mapping, where grayscale color was transformed to a blue-green-yellow-red color scale. The regions with a red color in the images represented hot spots, the regions with a blue color represented cold spots, and the regions with green and yellow colors represented areas in-between the cold and hot spots (Zhang et al., 2014). The color value of each pixel ranged from the minimum 0 to the maximum 255 (Fig. 4C). The average color values of the pixels inside the small reigns (in 10 mm diameter) at cold and hot spots were 21 and 213, respectively, for the RFG sample, and 78 and 217 for the RG sample. The cold spot was located at the points (24, 0) mm in the RFG sample and (0, 0) mm in the RG sample; the hot spots were at (0, 44) mm and (0, 55) mm in the RFG and RG samples, respectively.

The RFG was a solid food which was heated by microwave energy and hot water with involvement of heat conduction inside the sample; while the RG sample was a food with solid immersed in water, it was heated with involvement of heat convection inside the sample during most of the heating time. The different heat transfer mechanisms caused the different heating patterns in the two samples. The average color values in the heating pattern images were 96 for the RFG sample and 147 for the RG sample (Fig. 4 A&B). This indicted that the RG sample, because of the faster heat convection in it, got more thermal treatment than the RFG sample. The heating pattern result from the medium-moisture RFG model food was similar to those of the high-moisture solid foods, such as mashed potato and whey protein gel model foods (Resurreccion et al., 2015, 2013; Luan, Tang, Pedrow, Liu, & Tang, 2016, 2013); this was a critical finding of this study. Medium and high-moisture foods with different formulations and water contents have different dielectric properties, which changes how the electric field component of microwave energy will interact with the food (Tang et al., 2002). In general, increasing the moisture content of a food will increase the dielectric constant and loss factor and decrease the penetration depth, resulting in a food that will heat faster, but potentially have more issues with non-uniform heating (Tang et al., 2002). The MATS was designed using single-mode cavities, which would, in theory, yield a consistent heating pattern in foods with different formulas and dielectric properties (Tang, 2015). Previously published research using model food systems to determine the heating pattern in MATS has only used high moisture foods; this study is the first to present data that confirms this theory and it shows that medium-moisture foods do have a similar heating pattern to high moisture foods.

Table 2
Kinetic parameters for color formation at 116, 121 and 126 °C for rice grain model food systems (3 replicates).

Color values	Temp. (C°)	Initial value (C_0)	Saturation value (C_∞)	Reaction rate (k) (10^{-3}1/min)	D-value calculated from k (min)	E_a (kJ/mol/K)	R^2	Z-value calculated from E_a
L*	116	77.1 ± 0.4	45 ± 3	18 ± 3	129 ± 22	112 ± 7	0.99	26 ± 2
	121	76.7 ± 0.4	47 ± 1	29 ± 3	79 ± 8			
	126	76.5 ± 0.5	48 ± 1	43 ± 4	54 ± 4			
a*	116	0.8 ± 0.2	25 ± 2	18 ± 2	130 ± 17	166 ± 40	0.95	18 ± 4
	121	1.3 ± 0.2	19.2 ± 0.3	44 ± 2	52 ± 3			
	126	1.5 ± 0.2	20.2 ± 0.3	64 ± 3	36 ± 2			
Gray scale	116	0.75 ± 0.01	0.42 ± 0.03	20 ± 3	112 ± 16	108 ± 5	0.99	27 ± 1
	121	0.74 ± 0.01	0.43 ± 0.01	32 ± 3	71 ± 7			
	126	0.74 ± 0.01	0.44 ± 0.01	47 ± 4	49 ± 4			
ΔE	116	2.6 ± 0.4	42.3 ± 0.5	54 ± 2	42 ± 2	122 ± 10	0.99	24 ± 2
	121	2.8 ± 0.5	41.3 ± 0.4	94 ± 4	24 ± 1			
	126	2.8 ± 0.6	41.6 ± 0.5	140 ± 9	16 ± 1			

Table 3
Kinetic parameters for color formation at 116, 121 and 126 °C for rice flour gel model food systems (3 replicates).

Color values	Temp. (C°)	Initial value (C_0)	Saturation value (C_∞)	Reaction rate (k) (10^{-3}1/min)	D-value calculated from *k* (min)	E_a (kJ/mol/K)	R^2	Z-value calculated from E_a
L*	116	70.9 ± 0.5	−67 ± 21	2 ± 4	1028 ± 17	260 ± 35	0.98	11 ± 2
	121	70.4 ± 0.4	15 ± 13	8 ± 2	294 ± 92			
	126	69.9 ± 0.4	29 ± 3	17 ± 2	138 ± 16			
a*	116	0.6 ± 0.4	27 ± 3	15 ± 3	157 ± 34	148 ± 23	0.98	20 ± 3
	121	0.9 ± 0.3	21.4 ± 0.7	31 ± 2	75 ± 6			
	126	1.1 ± 0.3	21.2 ± 0.3	46 ± 2	50 ± 3			
Gray scale	116	0.68 ± 0.01	−0.13 ± 0.55	4 ± 3	528 ± 42	197 ± 17	0.99	15 ± 1
	121	0.67 ± 0.01	0.21 ± 0.07	11 ± 2	217 ± 48			
	126	0.67 ± 0.01	0.29 ± 0.02	20 ± 2	115 ± 11			
ΔE	116	1.5 ± 0.5	41.0 ± 0.5	52 ± 2	44 ± 2	95 ± 4	0.99	31 ± 2
	121	1.6 ± 0.3	39.7 ± 0.3	77 ± 2	30 ± 1			
	126	1.5 ± 0.4	40.1 ± 0.1	108 ± 3	21 ± 1			

In order to help confirm the accuracy of the cold and hot spot locations determined by the computer vision method, temperatures were measured by wireless temperature sensors at both locations during MATS processing (Fig. 5). After being preheated to 60 °C, the samples were moved through the microwave heating section and heated up to above 116 °C in 5.5 min. Then the samples passed through the holding section in 7 min and got enough thermal treatment. Finally, they were moved to the cooling section for cooling down. The time-temperature profiles of the hot and cold spots confirmed the hot spot received a more severe thermal treatment compared to the cold spot. Both the hot and cold spots in the RG model reached higher temperature than the RFG, which agrees the color difference in the heating pattern images for

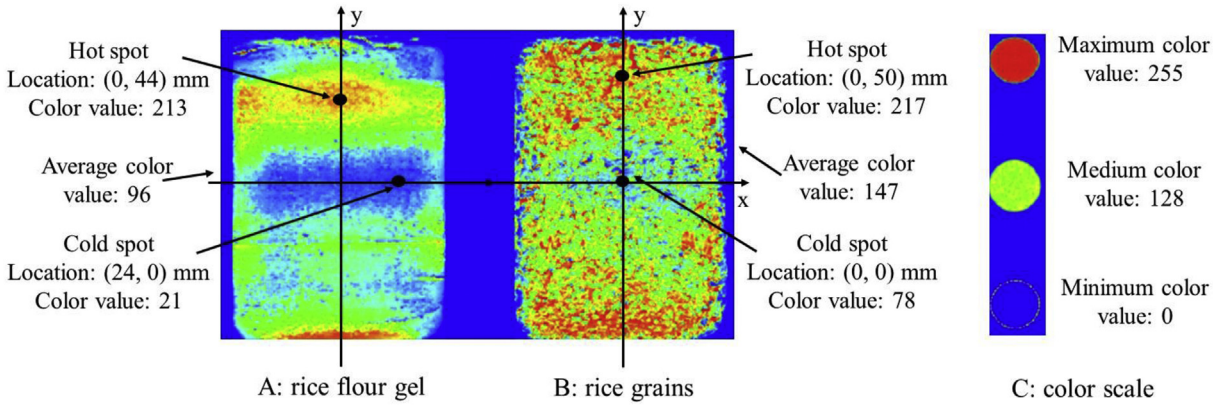

Fig. 4. Heating patterns visualized using color mapping for rice flour gel (A) and rice grain (B) model foods (0.5 g/100 g D-ribose, 0 g/100 g salt) after microwave assisted sterilization. The dark blue color in the color map (C) represents the least thermal treatment and least amount of color change, while the dark red color represents the most thermal treatment and largest amount of color change. (For interpretation of the references to color in this figure legend, the reader is referred to the Web version of this article.)

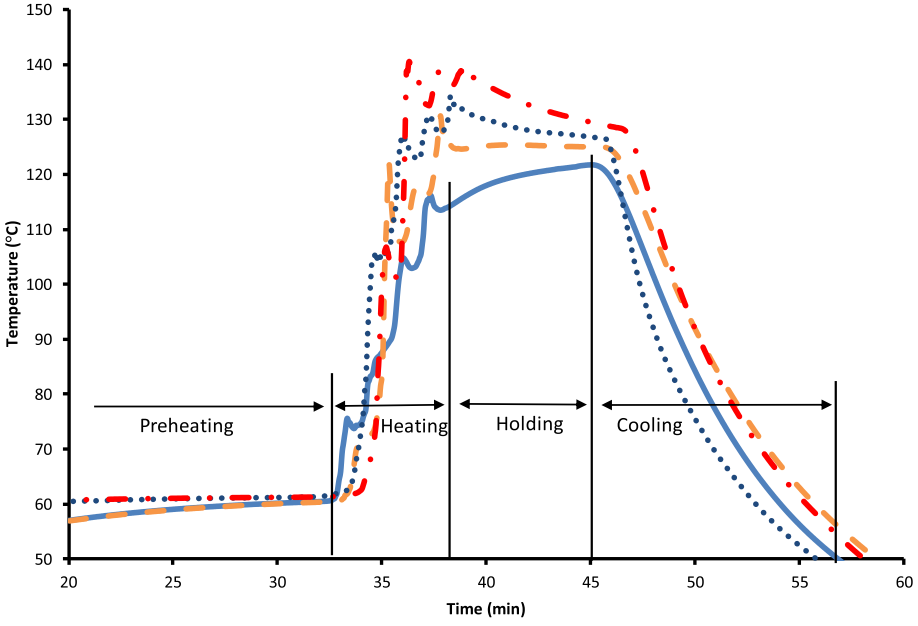

Fig. 5. Time-temperature profiles of the rice flour gel model food at the cold spot (——) and hot spot (– – – –), and rice grains model food at the cold spot (·····) and hot spot (– · – · –) during microwave assisted thermal sterilization.

the two samples (Fig. 5). Thermal lethality calculations confirmed that the cold spots in both foods received adequate thermal treatment to be considered thermally sterilized, with the RG and RFG model foods receiving a thermal treatment equivalent of 60.3 and 6.5 min at 121 °C, respectively. These promising validation results indicated that both rice model food systems could be used to visualize the heating pattern and locate hot and cold spots in medium-moisture food products processed in the microwave assisted thermal sterilization system.

4. Conclusion

The optimal composition of a rice flour gel (RFG) model food for sterilization temperatures was 30 g/100 g rice flour, 13.5 g/100 g tapioca starch, 0.1 g/100 g xanthan gum, and 0.5 g/100 g D-ribose. For a rice grain (RG) model food, the optimal composition was a rice to water ratio of 1:1.2 g/g with 0.5 g/100 g D-ribose. Color parameters (L*, a*, grayscale, and ΔE) followed first order reaction kinetics, and temperature dependence followed an Arrhenius relationship. For all temperatures and color parameters, the RG model food had slower color formation and smaller D-values compared to the RFG model food, which could be explained by differences in formulation and availability of reactants. The temperature sensitivity of the color parameters in the rice model food systems could be applicable for both safety and quality determination; the RFG model had a larger range of z-values (11–31 °C) than the RG model (18–27 °C). This study used multiple color components (L*, a*, grayscale, and ΔE) during image analysis; this approach differed from previous microwave-assisted thermal sterilization work that only considered grayscale value. During the validation studies, the RG model food heated at a faster rate and received more thermal treatment than the RFG model food, with RG and RFG model foods receiving thermal treatment equivalents at 121 °C of 60.3 and 6.5 min, respectively. This difference is likely due to variations in the heat transfer mechanisms inside the packages. The heating pattern and locations of cold and hot spots from the medium-moisture RFG model food was similar to those obtained in previous work using high-moisture model foods, which was a critical finding of this study. This is the first study to present data on medium-moisture foods processed in MATS and these results imply that the heating patterns in food packages processed in the MATS system would be consistent for both medium and high moisture foods that have similar consistencies. The rice model foods developed in this research could be useful in the future to visualize the heating pattern and locate cold and hot spots during the development of microwave assisted thermal sterilization processes for medium moisture foods, such as rice or pasta.

Acknowledgements

This research was supported by the Thailand Research Fund (TRF) and Charoen Pokphand Foods Public Co., Ltd. (Thailand) under “Research and Researchers for Industry Program (RRI)” [grant number PHD57I0057]. The authors also acknowledge partial support of USDA AFRI 2016-68003-24840.

Appendix A. Supplementary data

Supplementary data related to this article can be found at http://dx.doi.org/10.1016/j.lwt.2018.05.054.

References

Auksornsri, T., Tang, J., Tang, Z., Lin, H., & Songsermpong, S. (2018). Dielectric properties of rice model food systems relevant to microwave sterilization process. *Innovative Food Science & Emerging Technologies, 45*, 98–105.

Bornhorst, E. R., Liu, F., Tang, J., Sablani, S. S., & Barbosa-Cánovas, G. V. (2017a). Food quality evaluation using model foods: A comparison study between microwave assisted and conventional pasteurization processes. *Food and Bioprocess Technology, 10*, 1248–1256.

Bornhorst, E. R., Tang, J., Sablani, S. S., & Barbosa-Cánovas, G. V. (2017b). Development of model food systems for thermal pasteurization applications based on Maillard reaction products. *LWT- Food Science and Technology, 75*, 417–424.

Bornhorst, E. R., Tang, J., Sablani, S., & Barbosa-Cánovas, G. V. (2017c). Green pea and garlic model food development for thermal pasteurization process quality evaluation. *Journal of Food Science, 82*, 1631–1639.

Bornhorst, E. R., Tang, J., Sablani, S., & Barbosa-Cánovas, G. V. (2017d). Thermal pasteurization process evaluation using mashed potato model food with Maillard reaction products. *LWT- Food Science and Technology, 82*, 454–463.

Byun, Y., Hong, S. I., Mangalassary, S., Bae, H. J., Cooksey, K., Park, H. J., et al. (2010). The performance of organic and inorganic coated retort pouch materials on the shelf life of ready-to-eat rice products. *LWT- Food Science and Technology, 43*, 862–866.

Chantaro, P., & Pongsawatmanit, R. (2010). Influence of sucrose on thermal and pasting properties of tapioca starch and xanthan gum mixtures. *Journal of Food Engineering, 98*, 44–50.

Chung, H. J., Birla, S. L., & Tang, J. (2008). Performance evaluation of aluminum test cell designed for determining the heat resistance of bacterial spores in foods. *LWT- Food Science and Technology, 41*, 1351–1359.

Cong, H., Liu, F., Tang, Z., & Xue, C. (2012). Dielectric properties of sea cucumbers (*Stichopus japonicus*) and model foods at 915 MHz. *Journal of Food Engineering, 109*, 635–639.

Crowhurst, D. G., & Creed, P. G. (2001). Effect of cooking method and variety on the sensory quality of rice. *Food Service Technology, 1*, 133–140.

Gupta, R., Mikhaylenko, G., Balasubramaniam, V. M., & Tang, J. (2011). Combined pressure-temperature effects on the chemical marker (4-hydroxy-5-methyl- 3(2H)-furanone) formation in whey protein gels. *LWT- Food Science and Technology, 44*, 2141–2146.

Holdsworth, S. D. (1997). *Thermal processing of packaged foods* (1st ed.). New York, NY: Blackie Academic and Professional.

Hunter, R. S. (1975). *Measurement of appearance* (1st ed.). New York, NY: Wiley-Interscience.

Kim, H. J., & Taub, I. A. (1993). Intrinsic chemical markers for aseptic processing of particulate foods. *Food Technology, 47*, 91–99.

Lau, H., Tang, J., Taub, I. A., Yang, T. C. S., Edwards, C. G., & Mao, R. (2003). Kinetics of chemical marker formation in whey protein gels for studying high temperature short time microwave sterilization. *Journal of Food Engineering, 60*, 397–405.

Leelayuthsoontorn, P., & Thipayarat, A. (2006). Textural and morphological changes of Jasmine rice under various elevated cooking conditions. *Food Chemistry, 96*, 606–613.

Luan, D., Tang, J., Pedrow, P. D., Liu, F., & Tang, Z. (2013). Using mobile metallic temperature sensors in continuous microwave assisted sterilization (MATS) systems. *Journal of Food Engineering, 119*, 552–560.

Luan, D., Tang, J., Pedrow, P. D., Liu, F., & Tang, Z. (2016). Analysis of electric field distribution within a microwave assisted thermal sterilization (MATS) system by computer simulation. *Journal of Food Engineering, 188*, 87–97.

Narkrugsa, W., & Saeleaw, M. (2009). The retrogradation of canned rice during storage. *KMITL Science and Technology Journal, 9*, 1–8.

Nawab, A., Alam, F., Haq, M. A., & Hasnain, A. (2016). Effect of guar and xanthan gums on functional properties of mango (*Mangifera indica*) kernel starch. *International Journal of Biological Macromolecules, 93*, 630–635.

Pandit, R. B., Tang, J., Liu, F., & Mikhaylenko, G. (2007b). A computer vision method to locate cold spot in foods during microwave sterilization processes. *Pattern Recognition, 40*, 3667–3676.

Pandit, R. B., Tang, J., Liu, F., & Pitts, M. (2007a). Development of a novel approach to determine heating pattern using computer vision and chemical marker (M-2) yield. *Journal of Food Engineering, 78*, 522–528.

Pandit, R. B., Tang, J., Mikhaylenko, G., & Liu, F. (2006). Kinetics of chemical marker M-2 formation in mashed potato-a tool to locate cold spots under microwave sterilization. *Journal of Food Engineering, 76*, 353–361.

Phanchaisri, B., Chandet, R., Yu, L. D., Vilaithong, T., Jamjod, S., & Anuntalabhochai, S. (2007). Low-energy ion beam-induced mutation in Thai jasmine rice (Oryza sativa L. cv. KDML 105). *Surface and Coatings Technology, 201*, 8024–8028.

Pongsawatmanit, R., & Srijunthongsiri, S. (2008). Influence of xanthan gum on rheological properties and freeze-thaw stability of tapioca starch. *Journal of Food Engineering, 88*, 137–143.

Resurreccion, F. P., Luan, D., Tang, J., Liu, F., Tang, Z., Pedrow, P. D., et al. (2015). Effect of changes in microwave frequency on heating patterns of foods in a microwave assisted thermal sterilization system. *Journal of Food Engineering, 150*, 99–105.

Resurreccion, F. P., Tang, J., Pedrow, P., Cavalieri, R., Liu, F., & Tang, Z. (2013). Development of a computer simulation model for processing food in a microwave assisted thermal sterilization (MATS) system. *Journal of Food Engineering, 118*, 406–416.

Sae-kang, V., & Suphantharika, M. (2006). Influence of pH and xanthan gum addition on freeze- thaw stability of tapioca starch pastes. *Carbohydrate Polymers, 65*, 371–380.

Sakai, N., Mao, W., Koshima, Y., & Watanabe, M. (2005). A method for developing model food system in microwave heating studies. *Journal of Food Engineering, 66*, 525–531.

Srichamnong, W., Thiyajai, P., & Charoenkiatkul, S. (2016). Conventional steaming retains tocols and γ-oryzanol better than boiling and frying in the jasmine rice variety Khao dok mali 105. *Food Chemistry, 191*, 113–119.

Tang, J. (2015). Unlocking potentials of microwaves for food safety and quality. *Journal of Food Science, 80*, 1776–1793.

Tang, J., Feng, H., & Lau, M. (2002). Microwave heating in food processing. In X. Young, & J. Tang (Eds.). *Advances in bioprocessing engineering* (pp. 1–44). Hackensack, NJ: World Scientific Publisher.

Tang, J., Liu, F., Patfiak K., & Eves, E. E., (2006). Apparatus and method for heating objects with microwaves. US Patent 7119313 B2.

Tang, Z., Mikhaylenko, G., Liu, F., Mah, J. H., Tang, J., Pandit, R., et al. (2008). Microwave sterilization of sliced beef in gravy in 7-oz trays. *Journal of Food Engineering, 89*, 375–383.
Wang, Y., Lau, M. H., Tang, J., & Mao, R. (2004). Kinetics of chemical marker M-1 formation in whey protein gels for developing sterilization processes based on dielectric heating. *Journal of Food Engineering, 64*, 111–118.
Wang, Y., Tang, J., Rasco, B., Wang, S., Alshami, A. A., & Kong, F. (2009). Using whey protein gel as a model food to study dielectric heating properties of salmon (*Oncorhynchus gorbuscha*) fillets. *LWT- Food Science and Technology, 42*, 1174–1178.
Wang, Y., Wig, T. D., Tang, J., & Hallberg, L. M. (2003). Dielectric properties of foods relevant to RF and microwave pasteurization and sterilization. *Journal of Food Engineering, 57*, 257–268.
World Food Situation (2016). FAO Rice market monitor. http://www.fao.org/economic/est/publications/rice-publications/the-fao-rice-price-update/en/, Accessed date: 16 October 2016.
Zhang, W., Liu, F., Nindo, C., & Tang, J. (2013). Physical properties of egg whites and whole eggs relevant to microwave pasteurization. *Journal of Food Engineering, 118*, 62–69.
Zhang, W., Luan, D., Tang, J., Sablani, S. S., Rasco, B., Lin, H., et al. (2015). Dielectric properties and other physical properties of low-acyl gellan gel as relevant to microwave assisted pasteurization process. *Journal of Food Engineering, 149*, 195–203.
Zhang, W., Tang, J., Liu, F., Bohnet, S., & Tang, Z. (2014). Chemical marker M2 (4-hydroxy-5-methyl-3(2H)-furanone) formation in egg white gel model for heating pattern determination of microwave-assisted pasteurization processing. *Journal of Food Engineering, 125*, 69–76.